The Almena, Kansas, Tornadic Storm of 3 June 1999: A Long-Lived Supercell with Very Little Cloud-to-Ground Lightning

EUGENE W. MCCAUL JR.

Universities Space Research Association, Huntsville, Alabama

DENNIS E. BUECHLER

University of Alabama in Huntsville, Huntsville, Alabama

STEPHEN HODANISH

NOAA/National Weather Service, Pueblo, Colorado

STEVEN J. GOODMAN

NASA Marshall Space Flight Center, Huntsville, Alabama

(Manuscript received 1 May 2001, in final form 23 July 2001)

ABSTRACT

The visual, radar, and lightning characteristics of a severe thunderstorm that spawned a large F3 tornado near Almena, Kansas, on 3 June 1999 are documented. The storm is interesting in that it made a transition from a low-precipitation to classic supercell then back to low-precipitation supercell again prior to dissipation after sunset. The storm remarkably produced only 17 cloud-to-ground lightning flashes during its 4.5-h lifetime, despite vertically integrated liquid (VIL) values reaching 95 kg m^{-2}, reflectivities of 50 dB*Z* or greater at altitudes of 14 km, and baseball-size hail at the surface. In contrast, total lightning rates inferred from a portable lightning detector during the large tornado were very high, approximately 100 per minute, as expected for a storm of this size and intensity.

1. Introduction

Observations of supercells have revealed that such storms often tend to evolve toward the heavy-precipitation (HP) end of the supercell morphology spectrum (Doswell and Burgess 1993; Moller et al. 1994). Furthermore, for the large, intense midlatitude supercells that produce significant tornadoes, rates of cloud-to-ground (CG) lightning, although quite variable, often rival or exceed about one flash per minute (see MacGorman 1993; MacGorman and Burgess 1994). In a study of 42 violent (F4–F5) tornado-producing supercells, Perez et al. (1997) found mean CG flash rates ranging from 0.2 up to 54.3 per minute, with only four storms showing mean flash rates smaller than 0.5 per minute.

On 3 June 1999, a large isolated supercell formed in northwest Kansas, lasted at least 4.5 h and produced a large F3 tornado near Almena before dissipating in extreme southern Nebraska. The storm was unusual in that it produced only 17 CG flashes during its entire lifetime (mean CG flash rate of 0.06 per minute, or less than 1 flash each 15 min, on average). Total flash rates for the storm, however, were much larger than the CG rate and imply a very large ratio of intracloud (IC) to CG lightning flashes. The storm also exhibited an unusual structural evolution, in that, following the demise of the large F3 tornado, the storm reverted from a classic supercell back to its earlier pretornado low-precipitation (LP; Bluestein and Parks 1983) form. The purpose of this paper is to document these electrical and structural features using photographs, radar imagery, and CG and total lightning flash data.

2. Meteorological conditions and data

Meteorological conditions were favorable for supercell thunderstorms over northern Kansas and Nebraska on the afternoon of 3 June 1999. Moderate southwest flow prevailed aloft, and warm, humid air was present at the surface, with afternoon temperatures near 33°–

Corresponding author address: Eugene W. McCaul Jr., Institute for Global Change Research and Education, 4950 Corporate Dr., Suite 200, Huntsville, AL 35806.
E-mail: mccaul@space.hsv.usra.edu

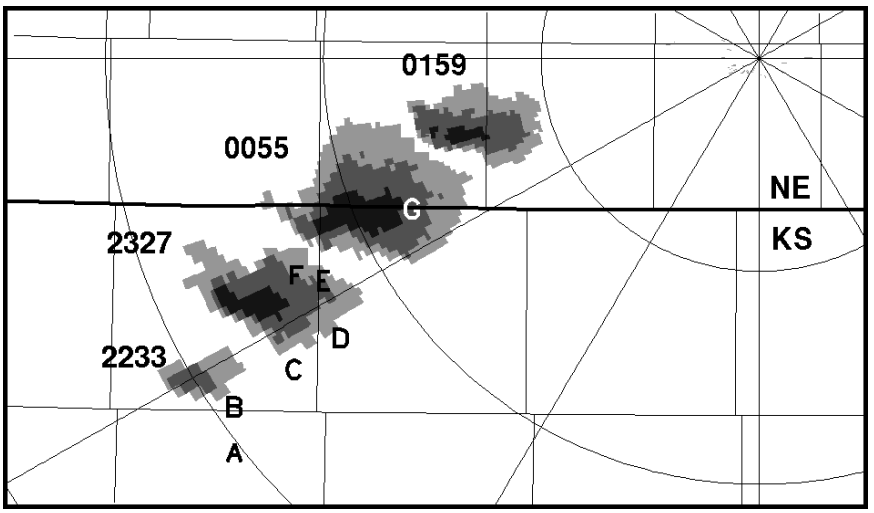

FIG. 1. Regional history of radar reflectivity (dBZ) evolution and trajectory for the Almena tornadic supercell, as seen in images sampled at the 0.5° elevation angle, from WSR-88D at Hastings, NE (KUEX). Reflectivity is shaded with increasing darkness in intervals of <35, 35–50 and >50 dBZ. Range rings are drawn at 50-km intervals. Times (UTC) are marked next to each radar image, and locations of the photos in Fig. 4 are also shown using letters A–G. All photos were made looking generally west through northwest, except for those made at locations F and G, which were made looking north through northeast.

35°C and dewpoints of 23°–25°C across northern Kansas. Surface winds were from the southeastern quadrant, except for Nebraska and extreme northern Kansas, where winds were backed just north of an outflow boundary caused by the passage of storms the previous night, and extreme western Kansas, where southwesterly flow prevailed behind a dryline. The Almena, Kansas, area is located roughly midway between sounding sites at North Platte, Nebraska, and Dodge City and Topeka, Kansas, so that a close proximity storm inflow sounding was not available. However, soundings from 0000 UTC 4 June 1999 from the above three sites indicated mean convective available potential energy (CAPE) values near 3000 J kg^{-1} and 0–3-km storm-relative helicity density values near 200 J kg^{-1}. Consideration of the surface conditions near the outflow boundary in the vicinity of Almena suggests that CAPE and helicity values may have been significantly larger in the near environment of the tornadic supercell.

The Almena storm developed near 2200 UTC 3 June just west of Hill City, Kansas, where it was intercepted by one of us (EWM), followed, and photographed until its demise around 0230 UTC 4 June near Alma, Nebraska. The photographs cover the storm's entire life cycle and are used to identify the various stages of visual morphology displayed by the storm. Doppler radar data from the National Weather Service (NWS) Weather Surveiliance Radar-1988 Doppler (WSR-88D) located at Hastings, Nebraska, (KUEX) were examined to analyze the evolving storm structure during the period from 2100 UTC 3 June to 0300 UTC 4 June. The entire CG lightning flash history of the storm was documented using data from the National Lightning Detection Network (NLDN; Cummins et al. 1998). A brief period of audio data from a portable total lightning detection unit was also available to document the total lightning behavior of the storm during part of its tornadic phase.

3. Results

A regional map illustrating the overall sequence of storm echo evolution and movement is given in Fig. 1. Based on the sequence of echo positions shown in the figure, the storm's mean motion was northeastward at a leisurely 6 m s^{-1}. The locations where the various photographs were made are also shown in Fig. 1. The storm formed in isolation and remained generally unaffected by other convective storms until the final hour of its life, when anvil cirrus from other newer storms in Nebraska began to impinge on it.

A series of eight reflectivity maps based on the lowest elevation (0.5°) angle data collected by KUEX between 2200 UTC 3 June and 0230 UTC 4 June is given in Fig. 2. The images are displayed in a coordinate frame

→

FIG. 2. Sequence of 60 km × 60 km radar reflectivity images (dBZ, shaded as in Fig. 1) sampled at 0.5° elevation angle, from WSR-88D at KUEX, for the life history of the Almena tornadic supercell. Times (UTC) are marked on each panel. Also shown are dotted lines indicating locations of vertical cross sections shown in Fig. 3.

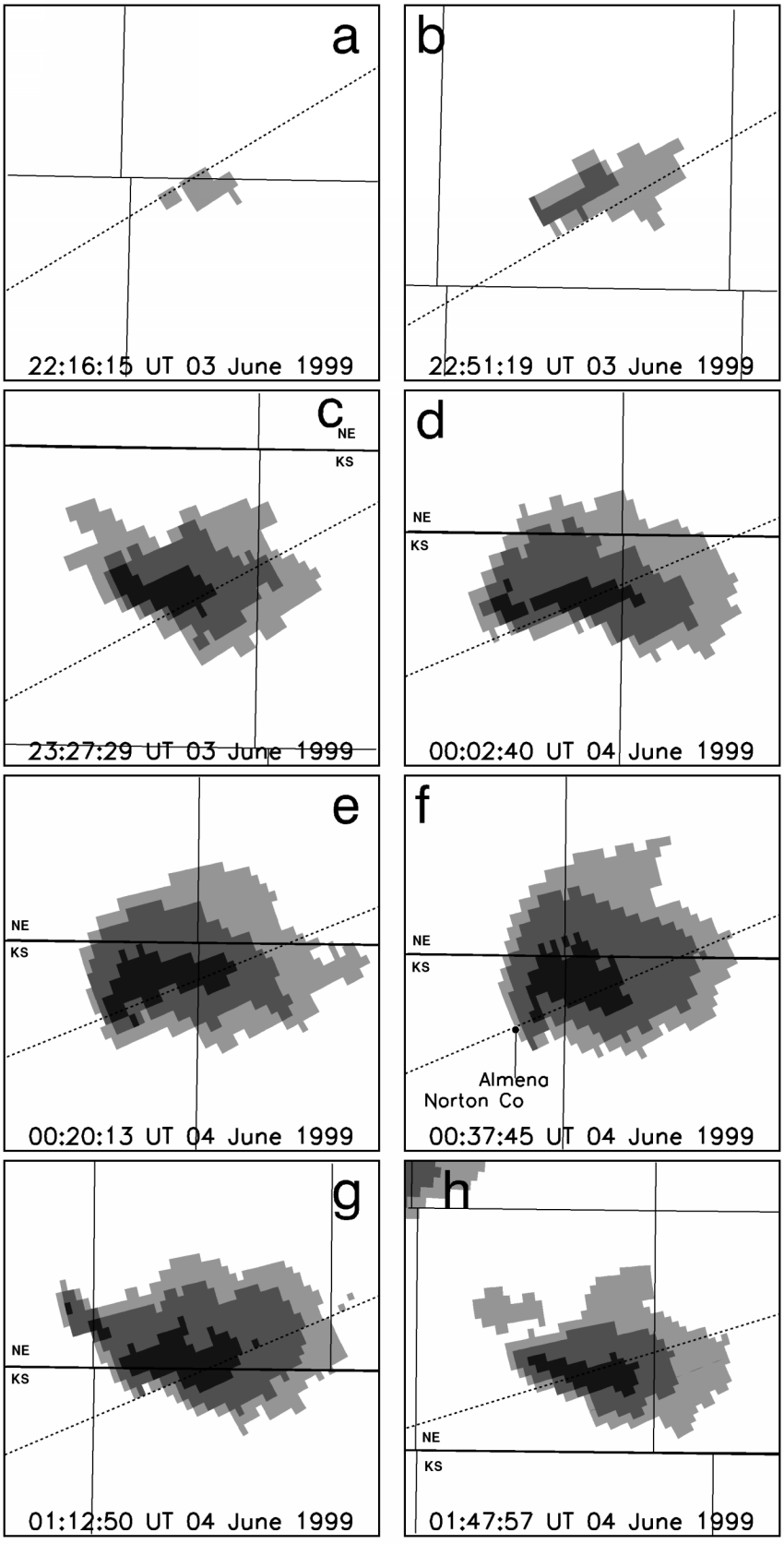

that follows the Almena storm. The storm formed at a location approximately 165 km southwest of the radar and dissipated at a location some 65 km west-southwest of it. The radar images generally show that the storm echo grew slowly in size for the first hour (Figs. 2a,b), then underwent an apparent splitting process by shedding echo material from its north flank (Fig. 2c), and then subsequently intensified to tornadic strength (Figs. 2d–f). Following the dissipation of the major tornado, the storm slowly weakened (Fig. 2g), and decreased in echo size (Fig. 2h).

A series of vertical cross-section plots of KUEX-derived reflectivity taken through the core of the Almena storm at the same nominal times of Fig. 2 are shown in Fig. 3. The locations of the cross sections are shown as dotted lines in the panels of Fig. 2, and all panels of Fig. 3 are shown with a view toward the north-northwest. The vertical growth of the reflectivity is readily apparent in Fig. 3, with large reflectivities regularly suspended at altitudes above 7 km during the mature phase of the storm. This gives some idea of the extreme intensity of the updrafts that were evidently present at mid- and upper levels of the storm.

A series of eight photographs (Fig. 4), spanning approximately the same time interval as the radar imagery in Fig. 2, shows that about 30 min after the first echo was detected from the growing tower (Fig. 4a), the Almena storm had developed a slender erect updraft and large anvil, but with no visible evidence of precipitation (Fig. 4b). At this time, the storm had the appearance of an LP supercell (Bluestein and Parks 1983; McCaul and Blanchard 1990). This LP phase of the storm continued until about 2300 UTC, when the updraft appeared to shed some cloud material off of its north side and reorganize (Fig. 4c). These weak north-flank echoes, which quickly decayed, are also seen in the radar reflectivity image in Fig. 2c. The raw version of Fig. 2c (not shown) contains a short north–south line of very weak echo returns attached to the western end of the main echo mass. We suspect this may be the signature of the dryline, which probably helped to trigger the storm.

A time series plot of radar-derived data indicates a sudden increase in vertically integrated liquid (VIL; Fig. 5) at about 2300 UTC. The time series of all NLDN-derived CG flashes for the Almena storm is also depicted in Fig. 5. It shows that the storm's first CG flash, which lowered negative charge to ground, occurred at 2310 UTC, shortly after the VIL first began to exceed 65–70 kg m^{-2}.

Just after 2300 UTC, the southern main updraft intensified and acquired a more obvious northeasterly tilt. By 2330 UTC the storm had completed the transformation into a more classic-type supercell, and a second negative-polarity CG flash (see Fig. 5) occurred.

By 2344 UTC another period of apparent updraft intensification was in progress, as evidenced by the photo in Fig. 4d and an increase in the storm's VIL to the very large value of 95 kg m^{-2} (see Fig. 5). This large VIL was associated with an updraft pulse that produced 57-dB*Z* reflectivities at altitudes of 14 km, which lay within the 6° elevation scan from KUEX. At this time the next elevation angle, 10°, showed no significant reflectivity. Following this outburst, VIL values remained large, often over 70 kg m^{-2} and occasionally above 80 kg m^{-2}, until about 0130 UTC (see Fig. 5). The large values of reflectivity at high altitudes throughout the mature phase of the supercell can also be seen in Fig. 3.

Between 2344 and 2351 UTC, a series of five CG flashes, three of positive polarity, were observed by NLDN (Fig. 4), and golfball-size (approximately 4.4 cm) hail was reported in Calvert, Kansas (NCDC 1999). Shortly after this, the first reports of weak tornado activity commenced near Norton, Kansas. After 2351 UTC, the CG activity decreased for at least 20 min, with only a single negative CG event near 0001 UTC. The KUEX radar image from 0003 UTC 4 June (Fig. 2d) shows the echo had developed a kidney-bean shape, in this case the precursor to a prolonged hook echo.

Between 0012 and 0018 UTC, four CGs, two of positive polarity, occurred at an almost even spacing in time (Fig. 5). During this interval, VIL increased again, reaching a second maximum of 83 kg m^{-2}. At 0018 UTC, a multiple-vortex tornado developed under the comma-head portion of the main updraft base, but dissipated quickly. By 0021, however, the tornado reappeared in the form of a large cone funnel. This tornado widened to at least 1 km during the next several minutes (Fig. 4e) and remained large and apparently intense until finally narrowing and roping out at 0047 UTC northeast of Almena. The tornado was frequently wrapped in rain curtains (Fig. 4f), and a well-defined hook echo was evident on radar throughout the tornado's lifetime (see Figs. 2e and 2f). Damage was limited to rural farmhouses, buildings, and powerlines but was substantial enough to warrant an F3 rating on the Fujita scale (NCDC 1999). The radar data indicate that the storm exhibited deviant right motion of approximately 20°–30° during its tornadic phase.

Although CG lightning was infrequent throughout the storm's lifetime, it was especially rare during the tornado, with only one negative-polarity flash at 0024 UTC (Fig. 5). However, larger overall CG and total lightning rates were expected during the mature phase of the storm, based on the amplitudes of the VIL and the altitudes to which strong reflectivity extended (Shafer and Carr 1990; Watson et al. 1995). Despite the near-absence of CG activity, there is evidence that the storm did at least produce considerable IC lightning at the time of the large tornado. A 14-min-long videotape recording made by one of us (SH) during the early stages of the large tornado documents the audible output from a portable total lightning detector, burst counts of which indicated lightning flashes occurring at a rate of approximately 100 per minute. During the same 14-min period, only two CG flashes were indicated by NLDN data. On

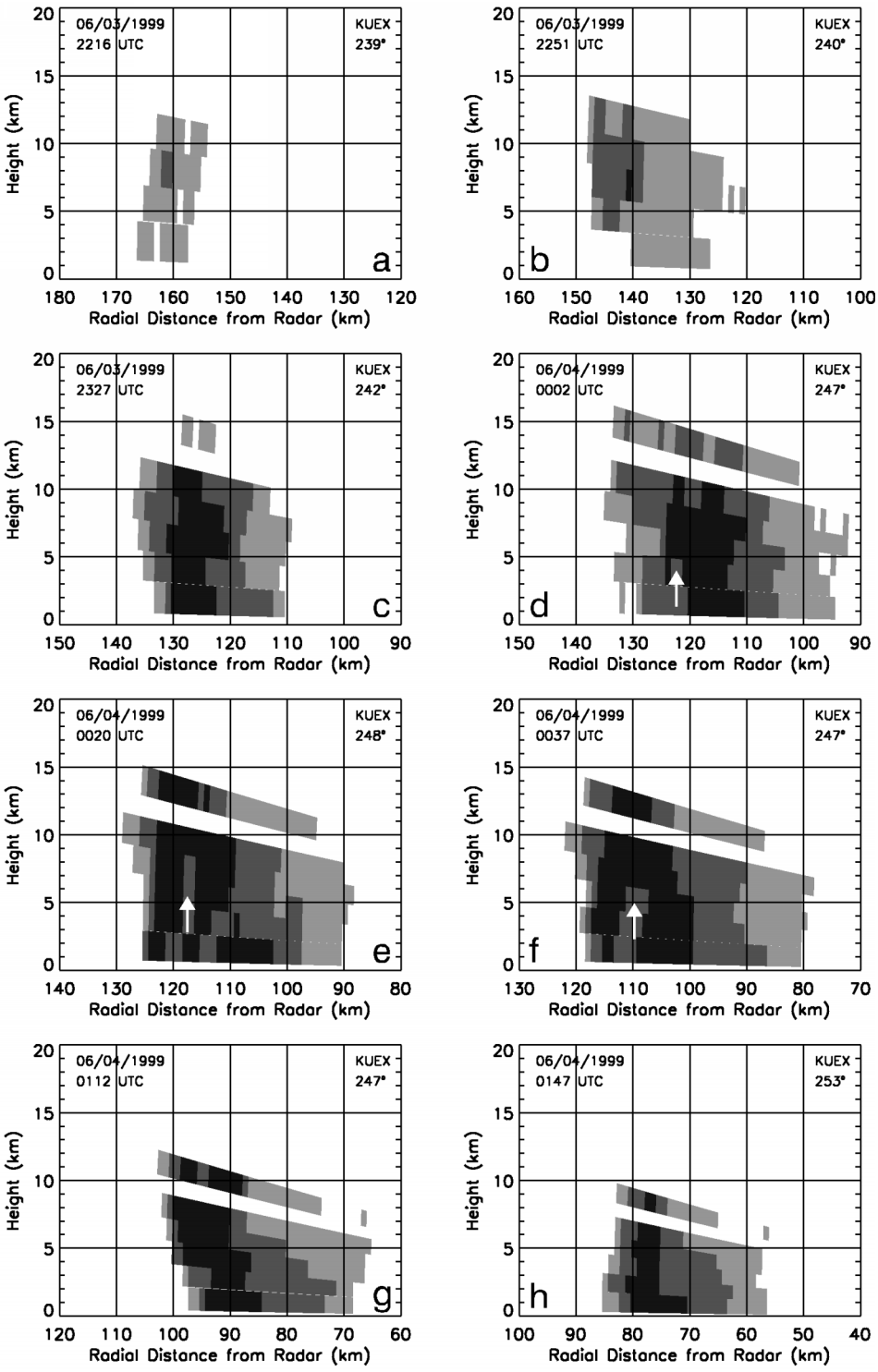

FIG. 3. Sequence of radar reflectivity cross sections (dBZ, shaded as in Fig. 1) as a function of range and height, from WSR-88D at KUEX, at the same times as shown in Fig. 2. View is to the north-northwest, along the section lines shown in the corresponding panels of Fig. 2. White arrows in (d), (e), and (f) denote location of vault in reflectivity field. Times are marked on each panel, and heights are measured relative to the altitude of KUEX.

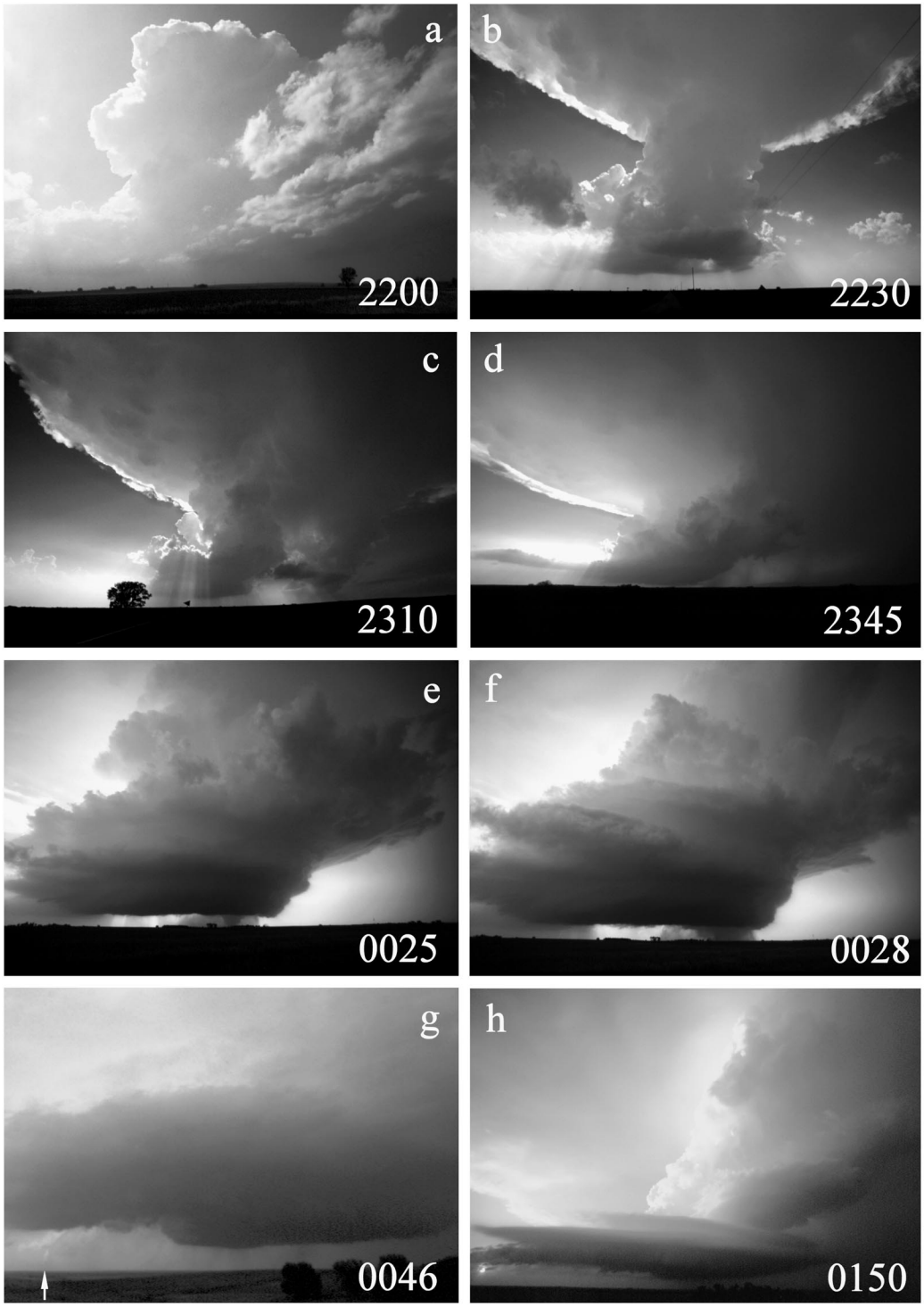

FIG. 4. Sequence of eight photographs of the Almena tornadic supercell. Approximate times (UTC) of photos are indicated. See Fig. 1 for locations at which the photographs were taken. Panel labels correspond to the labels of photograph locations in Fig. 1, except for (f), made at location E; (g) made at location F; and (h) made at location G. The storm is immature in (a), exhibits LP supercell structure in (b), then classic structure in (c)–(g), before finally reverting back to LP form in (h). In (g), the rope stage of the tornado is indicated by the arrow. All photographs are copyright 1999 by E. W. McCaul Jr.

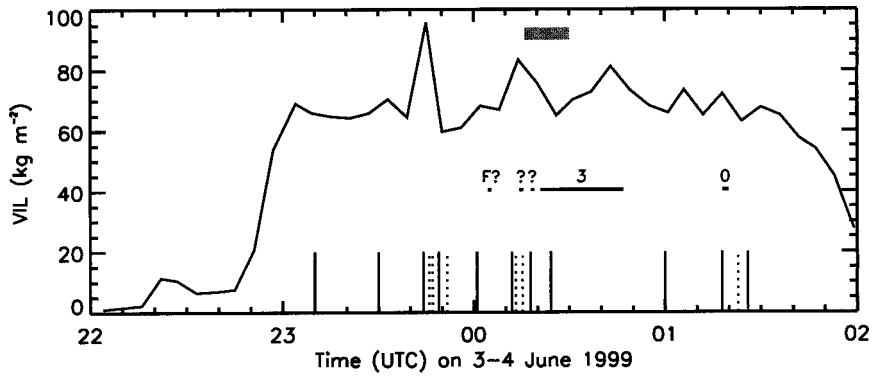

FIG. 5. Times series of KUEX Doppler radar-derived VIL (line plot), NLDN-derived CG lightning flashes (vertical lines, with positive polarity dashed), and tornado events (horizontal lines) for the Almena tornadic supercell. Shaded horizontal bar indicates the time interval for which videotaped total lightning flash data were available. Tornado events are labeled with numbers corresponding to F-scale ratings wherever available; the symbol ''?'' is used for unrated tornado events.

this basis, it appears that the storm achieved an IC:CG flash-rate ratio of 700, at least during the early stage of the large tornado.

The performance of the portable lightning detector appeared to be quite reliable, based on nocturnal observations of a frequent IC lightning-producing storm several days prior to the Almena storm, for which an excellent correlation between bursts of audible detector output and visible flashes of lightning was noted. This performance is consistent with the manufacturer's specifications for the instrument (R. Markson 2001, personal communication), when used to examine an isolated supercell storm from viewing ranges on the order of 10 km. The detector, a test prototype for a later model called the M-10, featured a field of view of 15° to reduce signals from extraneous storms, an 8-ms signal acceptance time lag to facilitate discrimination of individual strokes in flashes, and sufficient sensitivity to detect flashes reliably out to ranges of 120 km or more in areas of good visibility similar to that which prevailed during the Almena storm event.

The lightning detector was pointing north through northeast at the storm during data collection, and its field of view encompassed not only the tornado, but also the lower levels and midlevels of the main updraft core. Although the entire storm and its anvil were not fully within the instrument's field of view, most lightning flashes tend to scatter light throughout the cloud (Thomason and Krider 1982), which increases the likelihood that any given flash will be detected by the instrument. However, it is possible that some weak, distant flashes were missed, and that some audible bursts from the detector may have corresponded to multiple flashes that overlapped in time. Thus the detector's measured total flash rate should be viewed as a conservative estimate. On the other hand, the storm was isolated at the time of the tornado, and was studied at relatively close range, so that all flashes detected by the instrument likely came only from the Almena storm.

An additional feature of interest in the photo in Fig. 4f is the smooth, almost tubular form of the main updraft tower at midlevels (at estimated altitudes of 4–7 km). This is shown in the upper right part of Fig. 4f. We are unaware of any other photographic documentation that might provide direct visual evidence of rotation in this laminar midlevel updraft feature.

By around 0046 UTC 4 June, the large tornado shriveled to a rope form (left center of Fig. 4g) and then dissipated. Shortly after 0100 UTC 4 June, the storm attempted to generate new tornadoes northeast of Almena, but with only a small, brief F0 spinup reported by chasers and spotters. Hailstones of maximum dimension 7.0 cm (baseball size) were noted around this time on the ground near Long Island, Kansas, and had been melting for an undetermined period of time before being measured. From 0117 to 0125 UTC, the storm generated its last three CG flashes, two of which were negative in polarity. The updraft of the storm became progressively more slender after this time, with a large lenticular foot, apparently devoid of precipitation, attached to its base. These visual characteristics are again similar to those found in LP supercells (Bluestein and Parks 1983; McCaul and Blanchard 1990). Radar reflectivity maps (Fig. 2h), VIL (Fig. 5), photos (Fig. 4h), and visual observations also show a decrease in precipitation from the storm by 0150 UTC 4 June. On the basis of both the visual and radar evidence, the storm appeared to reacquire LP character late in its life. The resumption of LP morphology appeared to be delayed somewhat in the radar data relative to the visual observations, most likely because of the time required for precipitation formed during the classic phase to completely fall out of the storm. During this final phase, the storm eventually moved northeastward into Nebraska and dissipated after 0230 UTC.

During much of the storm's life, especially after the large tornado, the south edge of the storm's radar echo tended to lie along a west-northwest to east-southeast line. This orientation is also close to the approximate orientation of the old surface outflow boundary mentioned earlier. It is thus possible that the storm and its tornado were triggered, influenced, and perhaps ultimately destroyed by the approach to, interaction with, and eventual passage across this boundary. Recent observational studies (Markowski et al. 1998; Rasmussen et al. 2000) have found strong evidence that the likelihood of tornadogenesis increases when supercells interact with such boundaries.

4. Discussion

The Almena storm was remarkable for a combination of reasons, namely its intensity, its very small CG flash output, and aspects of its visual and radar evolution. One aspect of the storm's intensity is well described by its VIL history. As it neared maturity, the Almena storm produced a precipitation core featuring grid VIL values up to 95 kg m^{-2}. These VIL values are among the largest that we have seen documented to date.

During its 4.5-h lifetime, the Almena storm produced several tornadoes, the strongest being the giant F3, but only 17 CG flashes. Of these 17 CGs, 5 occurred in a 7-min period before the first weak tornadoes and large hail, and 4 more occurred in a 6-min period before the largest tornado. A narrow majority of these pretornado CGs were positive in polarity, but most of the CGs during the other parts of the storm's life were negative. The sparseness of the CG lightning makes it difficult to make a compelling case for polarity changes, but only one of five CGs occurring after the beginning of the large tornado was positive, suggesting a possible trend toward negative CG polarity following the onset of the large tornado. Such CG polarity changes have been noted during and after tornadoes in many other plains supercells (e.g., MacGorman 1993; Seimon 1993; MacGorman and Burgess 1994).

With its 17 CGs distributed more or less evenly throughout a 4.5-h period, the Almena storm exhibited a mean CG flash rate of only 0.06 per minute. This rate is 3 times smaller than the smallest reported by Perez et al. (1997), in their survey of 42 violent tornado–producing supercells. It is also nearly 3 orders of magnitude smaller than the mean CG flash rate displayed by the most active storm studied by Perez et al. (1997), the New Haven–Camden, Connecticut, supercell of 10 July 1989.

As noted earlier, the sparsity of CG activity in the Almena storm led to IC:CG ratios near 700 during the beginning phase of the large tornado. It is difficult to compare this IC:CG ratio with the few ratio measurements reported by other investigators from other storm events because of the incompleteness of our IC data record and because of differences in the way such ratios have been computed. Williams et al. (1999; their Table 2) found IC:CG ratios in the 22 February 1998 Florida tornadic supercells that reached maximum values of approximately 200; in our case, we cannot be sure that our 14-min period of IC data was coincident with the Almena storm's peak IC:CG flash ratio. Buechler et al. (2000) used satellite sensors in conjunction with NLDN data to estimate IC:CG flash-rate ratios of roughly 20 in a tornadic supercell in Oklahoma on 17 April 1995. Krehbiel et al. (2000) observed continuous IC lightning in an Oklahoma supercell on 8 June 1998, along with CG flash rates of 4 per minute. For their storm, the IC:CG ratio was likely phenomenally large, but aggregation of the raw radiation source data into discrete IC flashes was not feasible, and even if it had been feasible, the resulting IC flash rate would have had to exceed 2800 per minute to produce a ratio larger than that for Almena. In any case, the large IC:CG ratio noted here for the Almena storm derives primarily from the sparseness of its CG activity. Significant lulls in CG activity have been seen in many other tornadic supercells, especially during tornadoes (e.g., MacGorman and Burgess 1994), but for the Almena storm, the CG flash rate remained small for the entire 4.5-h lifetime of the storm.

The reasons for the sparsity of CG flashes from the Almena storm are unclear but may have to do with the storm's dynamical intensity, its tendency toward LP supercell morphology, and also with its isolation from other storms and from cirrus clouds. It has been suggested (Branick and Doswell 1992) that supercell morphology and electrification may be influenced by the impingement of cirrus clouds on a storm. They found that in the tornado outbreak of 13 March 1990 supercells tended more toward the HP end of the supercell spectrum and produced mostly negative-polarity CG flashes, to the extent they were immersed in suptropical jetstream cirrus. Other investigators (Buechler et al. 1996) have speculated that similar effects on storm morphology and electrification might also be produced by impingement of cirrus from the anvils of neighboring storms. No cirrus from other storms or from jetstream flow was ever observed to impinge on the Almena storm's updraft at any time during its life, although anvil material from new northern storms eventually did begin to merge with the Almena storm's anvil as it dissipated near sunset (Fig. 4h). The Almena storm's history of forming near the dryline and remaining isolated may also help to explain its morphological evolution. The switch from classic form back to LP late in the storm's life may simply be an example of what would be a common mode of dissipation of an isolated supercell but one not commonly witnessed visually, because most supercells either dissipate after dark, are obscured by low clouds after crossing boundaries, or interact with other storms and evolve toward the HP end of the supercell spectrum prior to dissipation.

5. Summary

The Almena tornadic supercell of 3–4 June 1999 constitutes an unusual case of supercell morphology changing from LP to classic and back to LP following a large tornado. Despite the fact that this large storm produced a long-lived and damaging tornado and achieved remarkably large VIL values during its maturity, it produced scant CG lightning, with only 17 flashes during a 4.5-h period. For this storm, NLDN data alone would not have been very useful to forecasters seeking to diagnose storm intensity. This behavior is reminiscent of the findings of Williams et al. (1999), Buechler et al. (2000), and others. From a lightning flash-rate point of view, the brief period of total lightning-rate data available to us indicates that total lightning data similar to those that could be derived from proposed satellite-based geostationary optical lightning sensors evidently would be needed to get a true picture of the overall intensity and intensity fluctuations of this kind of storm.

Acknowledgments. The NASA Headquarters Earth Science Enterprise supported this research. In particular, we acknowledge funding from NRA-99-OES-04, ''Investigations that Contribute to the NASA Earth Science Enterprise's Modeling and Data Analysis Research,'' sponsored by Dr. James Dodge. Additional support was provided by the NWS Forecast Office at Pueblo, Colorado.

REFERENCES

Bluestein, H. B., and C. R. Parks, 1983: A synoptic and photographic climatology of low-precipitation severe thunderstorms in the southern plains. *Mon. Wea. Rev.,* **111,** 2034–2046.

Branick, M. L., and C. A. Doswell III, 1992: An observation of the relationship between supercell structure and lightning ground-strike polarity. *Wea. Forecasting,* **7,** 143–149.

Buechler, D. E., S. J. Goodman, E. W. McCaul Jr., and K. R. Knupp, 1996: Cloud-to-ground lightning activity within tornadic storms in the Tennessee Valley. Preprints, *18th Conf. on Severe Local Storms,* San Francisco, CA, Amer. Meteor. Soc., 499–503.

——, K. T. Driscoll, S. J. Goodman, and H. J. Christian, 2000: Lightning activity within a tornadic thunderstorm observed by the Optical Transient Detector (OTD). *Geophys. Res. Lett.,* **27,** 2253–2256.

Cummins, K. L., M. J. Murphy, E. A. Bardo, W. L. Hiscox, R. B. Pyle, and A. E. Pifer, 1998: A combined TOAA/MDF technology upgrade of the U.S. National Lightning Detection Network. *J. Geophys. Res.,* **103,** 9035–9044.

Doswell, C. A., III, and D. W. Burgess, 1993: Tornadoes and tornadic storms: A review of conceptual models. *The Tornado: Its Structure, Dynamics, Prediction, and Hazards,* C. R. Church, Ed., Amer. Geophys. Union, 161–172.

Krehbiel, P. R., R. J. Thomas, W. Rison, T. Hamlin, J. Harlin, and M. Davis, 2000: GPS-based mapping reveals lightning inside storms. *Eos, Trans. Amer. Geophys. Union,* **81,** 21.

MacGorman, D. R., 1993: Lightning in tornadic storms: A review. *The Tornado: Its Structure, Dynamics, Prediction, and Hazards,* C. R. Church, Ed., Amer. Geophys. Union, 173–182.

——, and D. W. Burgess, 1994: Positive cloud-to-ground lightning in tornadic storms and hailstorms. *Mon. Wea. Rev.,* **122,** 1671–1697.

Markowski, P. M., E. N. Rasmussen, and J. M. Straka, 1998: The occurrence of tornadoes in supercells interacting with boundaries during VORTEX-95. *Wea. Forecasting,* **13,** 852–859.

McCaul, E. W., Jr., and D. O. Blanchard, 1990: A low-precipitation cumulonimbus along the dryline in Colorado. *Mon. Wea. Rev.,* **118,** 2768–2773.

Moller, A. R., C. A. Doswell III, M. P. Foster, and G. R. Woodall, 1994: The operational recognition of supercell thunderstorm environments and storm structures. *Wea. Forecasting,* **9,** 327–347.

NCDC, 1999: *Storm Data.* Vol. 41, No. 6, 324 pp.

Perez, A. H., L. J. Wicker, and R. E. Orville, 1997: Characteristics of cloud-to-ground lightning associated with violent tornadoes. *Wea. Forecasting,* **12,** 428–437.

Rasmussen, E. N., S. Richardson, J. M. Straka, P. M. Markowski, and D. O. Blanchard, 2000: The association of significant tornadoes with a baroclinic boundary on 2 June 1995. *Mon. Wea. Rev.,* **128,** 174–191.

Seimon, A., 1993: Anomalous cloud-to-ground lightning in an F5-tornado-producing supercell thunderstorm on 28 August 1990. *Bull. Amer. Meteor. Soc.,* **74,** 189–204.

Shafer, M. A., and F. H. Carr, 1990: Cloud-to-ground lightning in relation to digitized radar data in severe storms. Preprints, *16th Conf. on Severe Local Storms,* Kananaskis Park, Alberta, Canada, Amer. Meteor. Soc., 732–737.

Thomason, L. W., and E. P. Krider, 1982: The effects of clouds on the light produced by lightning. *J. Atmos. Sci.,* **39,** 2051–2065.

Watson, A. I., R. L. Holle, and R. E. Lopez, 1995: Lightning from two national detection networks related to vertically integrated liquid and echo-top information from WSR-88D radar. *Wea. Forecasting,* **10,** 592–605.

Williams, E., and Coauthors, 1999: The behavior of total lightning activity in severe Florida thunderstorms. *Atmos. Res.,* **51,** 245–265.